33rd Annual International Conference of the IEEE EMBS
Boston, Massachusetts USA, August 30 - September 3, 2011

Experimental Validation of a Reach-and Grasp Optimization Algorithm Inspired to Human Arm-Hand Control

F. Cordella, L. Zollo, *Member, IEEE*, A. Salerno,
E. Guglielmelli, *Senior Member, IEEE*, B. Siciliano, *Fellow, IEEE*

Abstract— Taking inspiration from neurophysiological studies on synergies in the human grasping action, this paper tries to demonstrate that it is possible to find a general rule for performing a stable, human-like cylindrical grasp with a robotic hand. To this purpose, the theoretical formulation and the experimental validation of a reach-and-grasp algorithm for determining the optimal hand position and the optimal finger configuration for grasping a cylindrical object with known features are presented. The proposed algorithm is based on the minimization of an objective function expressed by the sum of the distances of the hand joints from the object surface. Algorithm effectiveness has preliminarily been tested by means of simulation trials. Experimental trials on a real arm-hand robotic system have then been carried out in order to validate the approach and evaluate algorithm performance.

I. INTRODUCTION

FINDING an optimal grasp configuration is a fundamental part of the grasp planning action performed by a robotic hand. The difficulty of realizing a natural, reliable and optimal grasp has prompted researchers to explore different methods for solving the problem. Studying and replicating human grasping strategies is one of the viable approaches, which is pursued in this paper.The study in [1] suggests that the control of hand postures involves a few postural synergies. By combining those primitives it is possible to generate the entire repertoire of movements performed by human beings. It has also been demonstrated that, during grasping, joint angles of the hand do not vary independently [2]. Hence, the number of active degrees of freedom (DOFs) strictly necessary for controlling the hand shape is smaller than the total number of DOFs of the hand. This entails the feasibility of retrieving general rules for finding grasp configuration algorithms with reduced computational costs.

The aim of this paper is to prove that the concept of posture synergies can also be applied to a robotic hand, thus providing the basis for finding an optimal grasp configuration always applicable to certain grasping conditions. The paper resorts to the neuroscientific studies in [3] for showing that the optimal hand configuration for grasping cylindrical objects is the one minimizing distances between the object surface and the finger joints of a robotic hand. The main expected benefit of the proposed approach is to reduce the dimension of the space of feasible grasp configurations [4] in order to simplify the complexity of the algorithm, thus avoiding loss of grasp efficiency.

It is assumed that two of the three factors that mainly affect the grasping action [5] are pre-defined, i.e. the object physical characteristics and the task to be performed. In particular, object physical characteristics (like shape and weight) affect the hand posture [6] since the pre-shaping phase [7]. Later, when the reaching phase starts, hand aperture increases. It gradually decreases while approaching the object to be grasped in order to mold the hand shape around the object [8]. In this paper an algorithm is proposed for determining the optimal hand configuration that fits cylindrical object characteristics and ensures a stable palmar grasp. The proposed method consists of an optimization algorithm able to provide hand position, after reaching, and finger joint configuration, after preshaping, in order to achieve a stable grasp. It is experimentally tested on a robotic arm-hand system, consisting of the MIT-Manus robotic arm [9] and the DLR-HIT-Hand II [10], during reach-and-grasp tasks of cylindrical objects. The paper is structured as follows: in Section II the algorithm for determining the optimal grasp configuration is presented; in Section III, the experimental setup is described, while the experimental results are reported in Section IV. Conclusions and directions for future work are proposed in Section V.

II. ALGORITHM FOR THE OPTIMAL GRASP CONFIGURATION

The developed approach for determining a human-like hand grasp configuration resorts to findings on human behavior in [3] and re-adapt them to an arm-hand robotic

[1]Manuscript received March 26, 2011. The research leading to these results has been partially supported by the DEXMART Large-scale integrating project, which has received funding from the European Community's Seventh Framework Programme (FP7/2007-2013) under grant agreement ICT-216239. The authors are solely responsible for its content. It does not represent the opinion of the European Community and the Community is not responsible for any use that might be made of the information contained therein. This work was also supported by BrainHand (Fusion of Brain Analysis and Bio-inspired Robot Control for Enhancing Manipulation Capabilities of a Prosthetic Hand), funded by the Center for Integrated Research of Università Campus Bio-Medico.
F. Cordella and B. Siciliano are with the Department of Computer and Systems Engineering, University of Naples Federico II, 80125 Naples, Italy (e-mail: {francesca.cordella, bruno.siciliano}@unina.it).
L. Zollo, A. Salerno and E. Guglielmelli are with the Laboratory of Biomedical Robotics and Biomicrosystems, Università Campus Bio-Medico, 00128 Rome, Italy (+39 06 225419610; e-mail: {l.zollo, antonino.salerno, e.guglielmelli}@unicampus.it).

system. In [3] it is shown that the optimal configuration for grasping a cylindrical object is the one that minimizes the sum of the distances between the hand joints and the object surface. Based on this assumption, the position of the carpometacarpal (CMC) joint (Fig. 1) that guarantees a stable grasp configuration is obtained by minimizing the following objective function: $f = \sum_{i=1}^{4}\sum_{j=1}^{3} dist_j^i(y,\alpha)$ (1)

- index i indicates the i-th finger (it ranges from 1, the index finger, to 4, the little finger) and j is the joint index, ranging from 1 (the metacarpophalangeal, MCP, joint) to 3 (the distal interphalangeal, DIP, joint);
- $dist_j^i(y,\alpha)$ is the distance of the j-th joint of the i-th finger from the object surface (red dotted line in Fig.1). This distance is a function of y, i.e. the CMC y-coordinate in the reference frame of Fig.1, and α, i.e. the inclination angle of the object rotation axis (see Fig. 2) with respect to the z-axis of the reference frame;
- r_{obj} is the object radius.

For the experiments reported in this paper, it is assumed that the object physical characteristics, i.e. position and shape, are a priori known.

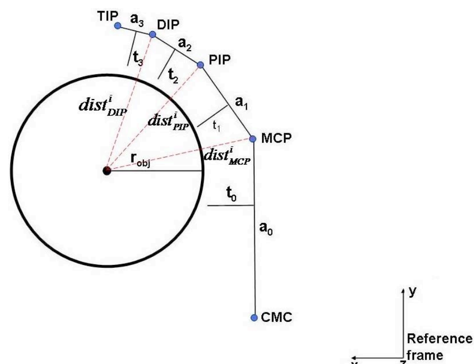

Figure 1: Schematic representation of the virtual scenario in which the algorithm has been developed.

As it is clear from Fig. 2, the fingers of a human hand are not parallel; they are inclined by certain angles. In order to account for such an inclination in the distance expressions in (1), a simpler case is first considered, in which the fingers are parallel to each other. Later, the extension to inclined fingers is proposed. In the case of parallel fingers, the planes where the fingers lie are perpendicular to the object rotation axis (the black line in Fig. 2). For each joint, the distances from the object surface can be expressed as:

$$dist^i_{MCP} = \sqrt{\left(y_{MCP_i} - y_{obj}\right)^2 + \left(r_{obj} + t_0\right)^2}, \quad (2)$$

$$dist^i_{PIP} = \sqrt{\left(a_1 - \sqrt{\left(r_{obj} + dist^i_{MCP}\right)^2 - \left(r_{obj} + t_1\right)^2}\right)^2 + \left(r_{obj} + t_1\right)^2}, \quad (3)$$

$$dist^i_{DIP} = \sqrt{\left(a_2 - \sqrt{\left(r_{obj} + dist^i_{PIP}\right)^2 - \left(r_{obj} + t_2\right)^2}\right)^2 + \left(r_{obj} + t_2\right)^2} \quad (4)$$

where:

- a_i is the finger link lengths and t_i is the finger thickness;
- y_{MCP_i} is the y-coordinate of the i-th finger MCP joint in the optimal configuration. Its value depends on the initial configuration ($y^{start}_{MCP_i}$ is the y-coordinate of the MCP joint in the start configuration) and on the inclination angle α given by the optimization procedure. In particular:

$$y_{MCP_i} = y + \left(y^{start}_{MCP_i} - y^{start}_{MCP_4}\right) + \left(z^{start}_{MCP_i} - z^{start}_{MCP_4}\right) * \tan\alpha \quad (5)$$

Figure 2: Human grasp of a cylindrical object. Fingers are tilted among themselves. The black line is the object rotation axis, the blue line is the rotation axis of the object in case it is inclined of a certain angle α. The reference frame is outlined in green.

Since it is assumed to work in the plane, the knowledge of the y-coordinate of the CMC and MCP joints is enough for computing the distance of the MCP joints to the object surface. Once doing that, it is possible to determine the joint x-coordinates. In order to have a 3D motion of the hand, the z-coordinate is imposed on the basis of considerations made in [11] and on the hand physical characteristics, as exposed in Section III. When fingers lie on planes inclined with respect to the plane perpendicular to the object rotation axis (plane xy in Fig. 1), joint projections in this plane are considered. These values are determined by replacing link length a_i, in the distance equations (2)−(4), with link length projections l_k computed by considering the vector normal to the xy-plane of Fig. 1. The length of the k-th finger link in the projection plane is given by:

$$l_k = a_k^2 - \left\| a_k \bullet \left(n_p \times n_o\right) \right\|^2 \bullet \left(n_p \times n_o\right)^2 + \left\| a_k \bullet \left(n_p \times n_o\right) \right\|^2 \quad (6)$$

where n_p is the normal vector to the plane perpendicular to the object rotation axis, n_o is the normal vector to the inclined plane where the finger lies and symbols $\bullet$ and $\times$ are respectively the dot and cross product. In this way it is possible to work in the projection plane, going back to the simplified case of parallel fingers. Thus, joint coordinates and angles determined in the projection plane are brought back to the original planes where the fingers lie. Joint Cartesian coordinates in the original plane are given by the intersection of that plane with the straight-line perpendicular to the original plane and passing through the joint in the projection plane. Joint angles are determined by means of inverse kinematics, starting from joint Cartesian coordinates. Through Eqs. (1) to (5), providing CMC y-coordinate and the distances of the joints from the object surface, in addition to some geometrical considerations, all the joint coordinates are computed and a human-like optimal grasp configuration is obtained.

III. EXPERIMENTAL SETUP

The algorithm described in Section II has been tested on a real arm-hand robotic system. The experimental platform (Fig. 3) used is composed of the MIT-Manus planar robot, which plays the role of the arm and realizes the reaching task, and the DLR-HIT-Hand II mounted at the MIT-Manus end effector, which is responsible for preshaping and grasping. The MIT-Manus system is a planar robotic arm (typically used for upper-limb rehabilitation) with two rotational degrees of freedom (i.e. DOFs), one for the elbow and one for the shoulder angular motion. It reproduces the planar motion of shoulder and elbow rotational joints of the upper limb in a workspace of 0.40x0.40 m. It is equipped with two optical encoders and a six-axis JR3 force/torque sensor. The five-fingered dexterous robotic hand DLR-HIT-Hand II has an independent palm and five identical modular fingers. Each finger has four DOFs, three actuated and one passive. The PIP and DIP joints are 1:1 coupled: the corresponding flexion/extension angles are equal. The thumb is mechanically constrained to assume a fixed opposition of 23.57 in the *xy*-plane with an inclination, with respect to *z*-axis, of 27.91; this only enables grasps with a fixed thumb inclination. The robotic fingers are inclined each other, as in the human hand. The middle finger is perpendicular to the object rotation axis. The angle between index and middle finger is 5°; while the angle of ring finger and little finger with respect to middle finger is 9°. Hand geometric parameters have been obtained by direct measurements on the robotic hand. A set of three cylinder with three different diameters (0.045 m, 0.047 m and 0.032 m, respectively) were selected. They have been used for: (i) extracting the optimal hand configurations for each object located in the working space by off-line running the optimization algorithm discussed Sect. II; (ii) carrying out the experimental tests of reach-and-grasp by means of the arm-hand robotic system. Fig. 3 shows the MIT-Manus reference frame $\left(x_{manus}, y_{manus}, z_{manus}\right)$, the DLR-HIT-Hand II reference frame $\left(x_{DLR}, y_{DLR}, z_{DLR}\right)$, the initial hand configuration, given in the MIT-Manus reference frame, and the object to grasp. Being the MIT-Manus planar, the arm and hand height from the table could not be varied. Therefore, the object has been properly located in order to allow closing the middle finger at half of the object height, coherently with studies on human beings in [11]. Once the object position has been provided to the optimization algorithm, the optimal CMC Cartesian position and the final hand configuration for grasping the object has been obtained by minimizing (1) through the MATLAB function *fminsearch (f, [initial condition])*. During reaching, the hand has been moved by the arm towards the optimal CMC position. Thus, the hand has been controlled in order to reach the final MCP, PIP, DIP joint angles, also provided by the algorithm. During reaching, the hand did not change orientation, being the arm motion planar: z_{DLR}-axis was parallel to y_{manus}.

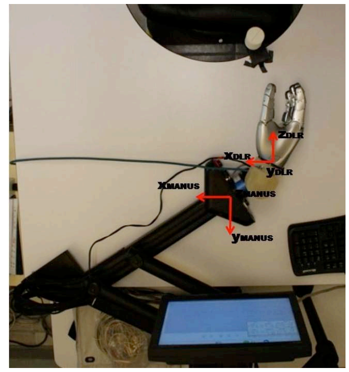

Figure 3: Experimental setup. The DLR-HIT-Hand II and MIT Manus reference frames are shown.

A fifth order polynomial function has been used to plan the MIT-Manus linear motion from the initial position (x=−0.1m, y=0.1m) up to the final position (x=−0.1m, y=−0.1m). Such final position has been determined by taking into account the CMC position supplied by the algorithm so as the offset between arm end effector and hand CMC due to the flange. Then, a proportional-derivative (PD) torque control in the Cartesian space has been used to control arm position (and consequently CMC position) in the plane. As regards preshaping, final joint positions, provided by the optimization algorithm, have been taken as reference for the robotic hand motion controller. A third-degree polynomial function has been used to plan joint motion up to the final reference value, and a PD torque control in the joint space has permitted reaching the desired final angles.

IV. EXPERIMENTAL RESULTS

The described algorithm was firstly tested in a simulated environment with the same characteristics of the real one, where MIT-Manus and DLR-HIT-Hand II kinematics were modeled. The obtained results, shown in Fig. 4, were encouraging, showing that fingers could properly grasp the object, as expected. Several experiments on real arm-hand robotic system were carried out in the working scenario described in Sect. III and shown in Fig. 3. A typical reach-and-grasp experimental trial lasted 4.2 s. During reaching, the MIT-Manus moved for 2 s along a straight line from initial position B=(-0.1,0.1)m to final point C=(-0.1,0.1)m. The corresponding CMC position coming out from the optimization algorithm, was (x= -0.055m, y= -0.1602m). The reaching movement was followed by 1s of settlement. Thus, grasping was performed by the hand in 1.2 s. The power grasp following preshaping performed by the arm-hand robotic system is shown in Fig. 5. The cylindrical object to be grasped had 0.0224 m radius and was located in (-0.051, -0.257) m in the MIT-Manus reference frame. Experimental results of the grasping phase are drawn in Fig. 6 showing the position error of MCP and PIP joints during preshaping. The experiment was repeated for cylinders of different radii. In particular three cases were tested: r_{obj}=0.0224m (case A), r_{obj}=0.0236m (case B), r_{obj}=0.0158m (case C).

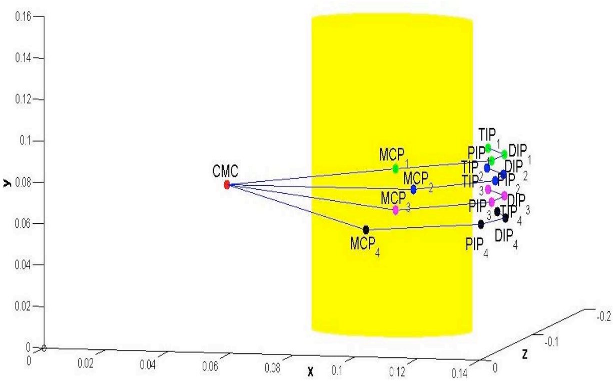

Figure 4: Plot of joint and object position. Joints are dotted.

In Table I the experimental results, in terms of optimal joint angle values given by the algorithm and effective angles actually reached by the DLR-HIT-Hand, are shown. The convention used in Table I, for each row, is:

$$\vartheta_{joint} = \left[\vartheta_{joint}^{index} \quad \vartheta_{joint}^{middle} \quad \vartheta_{joint}^{ring} \quad \vartheta_{joint}^{little} \right],$$

where subscript *joint* can be MCP or PIP.

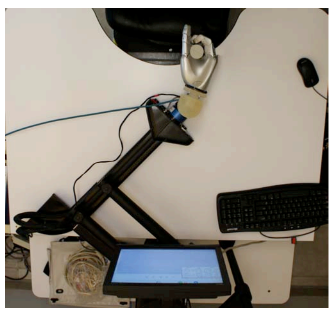

Figure 5: Grasping action completed

TABLE I
EXPERIMENTAL RESULTS

Case analyzed	Optimal joint angle (degrees)	Effective joint angle (degrees)
A	$\vartheta_{MCP} = [61.4 \quad 74.6 \quad 67.4 \quad 44.1]$	$\vartheta_{MCP} = [55 \quad 65 \quad 65 \quad 30]$
	$\vartheta_{PIP} = [49.8 \quad 38.9 \quad 45.5 \quad 55.1]$	$\vartheta_{PIP} = [55 \quad 48 \quad 50 \quad 60]$
B	$\vartheta_{MCP} = [45 \quad 47 \quad 44 \quad 45]$	$\vartheta_{MCP} = [45 \quad 57 \quad 48 \quad 30]$
	$\vartheta_{PIP} = [47.8 \quad 37.4 \quad 43.6 \quad 52.9]$	$\vartheta_{PIP} = [45 \quad 47 \quad 44 \quad 45]$
C	$\vartheta_{MCP} = [66.7 \quad 81.2 \quad 73.4 \quad 47.2]$	$\vartheta_{MCP} = [60 \quad 84 \quad 70 \quad 36]$
	$\vartheta_{PIP} = [63.4 \quad 49.9 \quad 58.1 \quad 69.8]$	$\vartheta_{PIP} = [60 \quad 60 \quad 60 \quad 70]$

It is worth observing that position errors between the algorithm optimal joint angles and actual finger joint angles in some cases reach values around 10°. The cause is the hand mechanical structure that does not allow completely reaching the desired joint configurations extracted by the optimization algorithm. This is related in particular to the fixed thumb opposition and to the 1:1 coupling of the PIP and DIP joints, while in humans the ratio between them seems to be around 2/3 [12]. The main consequence is that for some objects (especially for large radii), the final fingertip (TIP) position calculated by the algorithm falls within the object, beyond the object surface. Within these mechanical limits, the hand performs a firm grip of the object.

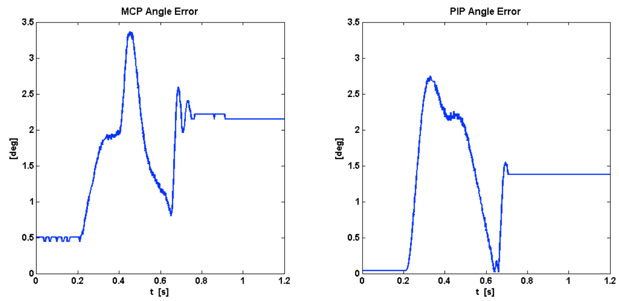

Figure 6: Plots of the MCP and PIP joint angle trajectory tracking error

V. CONCLUSION

A biologically inspired approach for finding the optimal grasp configuration has been presented, with special attention to the final position of the reaching movement and the optimal finger configuration for a power grasp. It was tested on a real arm-hand robotic system, composed of the MIT-Manus robot arm and the DLR-HIT-Hand II. The proposed method is based on recent findings on human behavior and provides a technique for grasping cylindrical objects with a human-like hand configuration that is general and applicable to anthropomorphic robotic hands. Experimental tests on the described robotic platform proved its feasibility and reliability.

REFERENCES

[1] M. Santello, M. Flanders, J.F. Soechting, "Postural hand synergies for tool use", *J. Neurosci.*, vol. 18, no. 23, pp.105−115, 1998.

[2] C.R. Mason, J.E. Gomez, T.J. Ebner, "Hand synergies during reach-to-grasp", *J. Neurophysiol*, vol. 86, no. 6, pp. 2896−2910, 2001.

[3] W. Lee, X. Zhang, "Development and evaluation of an optimization-based model for power-grip posture prediction", *Journal of Biomechanics*, vol. 38, pp. 1591−1597, 2005.

[4] M.A. Roa, R. Suarez, "Regrasp planning in the grasp space using independent regions", *2009 IEEE/RSJ International Conference on Intelligent Robots and Systems*, pp. 1823−1829, 2009.

[5] C. L. Mackenzie, T. Iberall, *The Grasping Hand*, Elsevier-North Holland, 1994.

[6] M. Santello, M. Flanders, J.F. Soechting, "Patterns of hand motion during grasping and the influence of sensory guidance", *J. Neurosci.*, vol. 22, no. 4, pp.1426−1435, 2002.

[7] M. Jeannerod, M.A. Arbib, G. Rizzolatti, H. Sakata, "Grasping objects: the cortical mechanisms of visuomotor transformation", *Trends Neurosci.*, vol. 18, pp. 314−320, 1995.

[8] M. Santello, J.F. Soechting, "Gradual molding of the hand to the object contours", *J. Neurophysiol.*, vol. 79, pp. 1307−1320, 1998.

[9] N. Hogan, H. I. Krebs, J. Charnnarong, P. Srikrishna, A. Sharon, "MIT-Manus: A workstation for manual theraphy and training", *1992 IEEE International Workshop on Robot and Human Communication*, pp. 161−165, 1992.

[10] H. Liu et al., "Multisensory five-finger dexterous hand: the DLR-HIT Hand II", *2008 IEEE/RSJ International Conference on Intelligent Robots and Systems*, pp. 3692−3697, 2008.

[11] J. Lukos, C. Ansuini, M. Santello, "Choice of contact points during multidigit grasping: effect of predictability of object center of mass location". *J. of Neurosci.*, vol. 27, no. 14, pp. 3894−3903, 2007.

[12] J. Lee, T.L. Kunii, "Model-based analysis of hand posture", IEEE Computer Graphics and Apllications, vol. 15, no. 5, pp. 77-86, 1995.